Control of physical interaction through tactile and force sensing during visually guided reaching

Lorenzo Jamone[1], Matteo Fumagalli[2], Lorenzo Natale[3], Francesco Nori[4], Giorgio Metta[3] and Giulio Sandini[4]

***Abstract*— In this paper we describe a control framework that integrates tactile and force sensing to regulate the physical interaction of an anthropomorphic robotic arm with the external environment. In particular, we exploit tactile sensors distributed on the robot fingers and a 6-axis force/torque sensor place at the bottom of the arm, just below the shoulder. Due to their different mounting locations and sensitivity, the sensors provide different types of contact information; their integration allows to deal with both slight and hard contacts by performing different control strategies depending on the location and the intensity of the contact. We provide real-world experimental results that show how a humanoid torso equipped with moving head, eyes, arm and hand can realize visually guided reaching dealing with different types of unexpected contacts with the environment.**

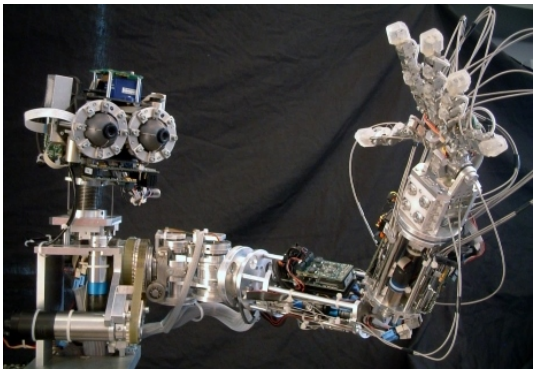

Fig. 1. The humanoid robot James.

I. Introduction

Autonomous robots are expected to coexist with humans, sharing their living and working environments, performing useful tasks while adapting to the surrounding space and reacting to unpredictable events. When a robot moves in an unknown and unstructured environment force and tactile information is of primary importance to deal with the risk of unexpected and unmodeled contacts with the environment. In those situations, compliance is fundamental in order to avoid damaging the robot and the surrounding environment (physical objects and/or interacting agents) during the movements. While passive compliance can be obtained including elastic elements within the mechanical structure of the robot, specific sensors that detect physical contacts with the environment (e.g. force/torque sensors, tactile sensors) can be used to realize active compliant behaviors.

State of the art performance can be obtained through either torque sensing on each joint [1] or variable impedance actuators (VIA) [1], [2]; however, both solutions require an highly integrated and advanced mechatronic design, that is currently not available on many robots, having high costs and complexity. An alternative, simpler and cheaper solution, is to put a single force/torque (FT) sensor along the robot kinematic chain. One possibility is to place a FT sensor on the end-effector, where most of the interactions occur [3]. However, external forces acting on the other parts of the arm cannot be measured with this configuration; furthermore, it may be problematic to put the sensor on the end-effector, due to its excessive size or weight. Another possibility is to place the sensor at the base of the manipulator or along the kinematic chain (e.g. after the shoulder) [4]–[7], allowing the robot to detect contacts with the environment not only on the end-effector, but on the whole arm. In this case, however, the FT sensor measures both external and internal forces, the latter being the ones depending on gravitational, Coriolis and inertial forces. In order to accurately detect the external contribution of the forces, the manipulator dynamics must be compensated for, i.e. the internal forces must be known, modeled or estimated. In case an artificial skin covering the robotic arm is available, the application point of the external force can be detected, improving the definition of the control inputs to control the interaction [8].

In this paper we propose to integrate the sensory information coming from different channels in order to control the physical interaction with the environment in different situations, executing different behaviors depending on the intensity and location of the contact, while taking in consideration the robot task. In particular, we show how the integration of visual, tactile and force/torque information allows to perform visually guided goal-directed reaching movements while dealing with unexpected contacts with the environment. A 6-axis force/torque sensor placed at the bottom of the arm kinematic chain (i.e. just after the shoulder) allows the robot to detect contacts occurring on the arm links, while tactile sensors distributed on the hand provide more specific information about contacts on the hand; additional information

*This work was partially funded by the EU Projects POETICON++ [FP7-ICT-288382] and LIMOMAN [PIEF-GA-2013-628315].

[1]L. Jamone is with the Instituto de Sistemas e Robótica, Instituto Superior Técnico, Universidade de Lisboa, Portugal. ljamone at isr.ist.utl.pt

[2]M. Fumagalli is with the Robotics and Mechatronics Group of the University of Twente m.fumagalli at utwente.nl

[3]L. Natale and G. Metta are with the iCub Facility, Istituto Italiano di Tecnologia, Genoa, Italy lorenzo.natale,giorgio.metta at iit.it

[4]F. Nori and G. Sandini are with the Department of Robotics, Brain and Cognitive Sciences, Istituto Italiano di Tecnologia, Genoa, Italy francesco.nori,giulio.sandini at iit.it

extracted from vision is used to specify whether the contact is caused by an obstacle that needs to be avoided or by successful reaching of the target object, triggering different reactive behaviors.

The rest of the paper is organized as follows. In Section II we describe the humanoid robot that we used for the experiments, and in Section III we explain how we combine the use of proximal force/torque sensing and the estimation of the robot dynamics to detect external forces and torques acting on the robot arm. Then, in Section IV we present experimental results showing how the integration of vision, tactile and force/torque sensing allows to control the physical interaction with the environment in the different situations, and in Section V we summarize our conclusions.

II. The robotic platform

The work described in this paper has been carried out using the humanoid robot James [9]. James is a humanoid torso, consisting of a 7 DOF head, a 7 DOF left arm and a 8 DOF left hand, with the overall size of a 10 years old boy (see Figure 1). A single 6-axis FT sensor (ATI mini45 [10]) is placed at the top of the upper arm, just below the shoulder. This placement allows to detect external forces applied to any point on the arm/hand surface, given that the internal forces generated by the arm motion (that are also detected by the sensor) are compensated for.

The hand of James is equipped with a total of 17 tactile elements, distributed on the internal side of each finger. Each tactile element consists of a small magnet immersed in a silicone part, that lies over an Hall-effect sensor. When a force is applied on the external side of the silicone part the magnet gets closer to the Hall-effect sensor, that detects a change in the magnetic field: this provides an indirect measure of the applied force. The sensing mechanism is described in more details in [9].

The torque generated by the motors is transmitted to the joints through plastic toothed belts and stainless-steel cables (i.e. tendons); additional mechanical compliance has been added by means of springs in series with some of the cables. On the one hand, this kind of actuation gives a noteworthy intrinsic compliance (i.e. passive compliance) to the system, easing the interaction over an unknown and unstructured environment; indeed, slight contacts with the environment can be absorbed by the elastic structure, avoiding damaging the robot and/or the environment. On the other hand, the presence of elastic elements (i.e. plastic belts, cables, springs) increases the complexity of the system, making very hard to obtain accurate analytical models for control; we solved this issue by heavily relying on learned models to control the system, as shown for example in the control of arm reaching [11] and neck orientation [12]. In particular, neck control also exploits force information extracted from an ad-hoc sensor [13], allowing active compliance as well.

III. Detection of external forces

As described in [6], [7], an FT sensor mounted within a kinematic chain measures both internal and external forces. The former refer to the forces and torques that are due to the sole dynamics of the robotic arm in an unconstrained motion. The latter are the forces and torques that are applied by the external environment and that must be determined for interaction control purpose (e.g. obstacle detection and avoidance). In the following we will discuss the retrieval of the external forces and the consequent need to estimate the internal ones.

Let us consider an open kinematic chain with n degrees of freedom. Let $\mathbf{q} \in \mathbb{R}^n$ be the generalized coordinates describing the pose of the kinematic chain. The FT sensor measurement will be denoted $\mathbf{x} = [\mathbf{f}^\top, \tau^\top]^\top \in \mathbb{R}^6$. As previously mentioned, this quantity contains both external and internal forces $\mathbf{f} \in \mathbb{R}^3$ and torques $\tau \in \mathbb{R}^3$. Specifically we have:

$$\mathbf{x} = \mathbf{x}_I + \mathbf{x}_E \ , \tag{III.1}$$

where $\mathbf{x}_I$ and $\mathbf{x}_E$ refer to the internal and external forces/torques, respectively. Without loss of generality, let us assume that we have the measurement of the load position of the joint $\mathbf{q}$, such that the dynamic model of the wrench measured by he sensor robot can be described as follows:

$$\begin{bmatrix}\mathbf{f}\\ \tau\end{bmatrix} = \underbrace{M_x(\mathbf{q})\ddot{\mathbf{q}} + C_x(\mathbf{q},\dot{\mathbf{q}})\dot{\mathbf{q}} + g_x(\mathbf{q})}_{\mathbf{x}_I} + \underbrace{T(\mathbf{q},\mathbf{d})\begin{bmatrix}\mathbf{f}_E\\ \tau_E\end{bmatrix}}_{\mathbf{x}_E} \ , \tag{III.2}$$

where $\mathbf{f}_E, \tau_E$ represent the external forces and torques applied at the point where the contact happens, $M_x \in \mathbb{R}^{6xn}$, $C_x \in \mathbb{R}^{6xn}$ and $g_x \in \mathbb{R}^{6xn}$ the inertial, Coriolis and gravity matrices of the dynamic system equations (with respect to the sensor reference frame) and T is a roto-translation matrix describing the transformation of the external forces from the contact point reference frame to the sensor reference frame, with $\mathbf{d}$ being the distance vector from the contact point to the sensor.

Whenever the robot interacts with an external object, a non-null external force component $\mathbf{x}_E$ arises: in order to detect a collision or a contact, $\mathbf{x}_E$ must be identified from the sensor measurements $\mathbf{x}$. Practically, the identification can be performed by subtracting the internal forces ($\mathbf{x}_I$) from the measured ones ($\mathbf{x}$):

$$\mathbf{x}_E = \mathbf{x} - \mathbf{x}_I \ , \tag{III.3}$$

which yields an indirect measurement of the external forces and torques. Then, the vector $\mathbf{x}_I$ must be computed from the model, or derived from experimental data. When the robot moves freely in its workspace, the sensor only perceives the internal components of forces and torques (i.e. $\mathbf{x}_I = \mathbf{x}$). These components only depend on position, velocity and acceleration of the joints. The problem of retrieving $\mathbf{x}_E$ is therefore reduced to the estimation of the internal forces and torques, i.e. the mapping from $\mathbf{q}, \dot{\mathbf{q}}, \ddot{\mathbf{q}}$ to $\mathbf{f}, \tau$:

$$\mathbf{x}_I = f(\mathbf{q}, \dot{\mathbf{q}}, \ddot{\mathbf{q}}). \tag{III.4}$$

A. Estimation of internal forces

Multiple approaches can be used to estimate the internal forces generated by the unconstrained motion of a robot arm, as detected by an FT sensor placed at its base. Firstly, the functional estimation can be done using an analytical model describing the physics of the system. Model-based estimation strongly relies on the availability of a (mathematical) model of the robot [14]: to this purpose, rigid multi-body dynamic modeling is generally used to identify the dynamic parameter of the robot [15], but the complexity of the identification drastically increases if the system cannot be considered as rigid. Within this context, the overall model accuracy is primarily limited by the (potentially nonlinear) effects which the model does not explicitly take into account (e.g. tendon elasticities).

Alternatively, supervised machine learning approaches can be used to approximate the internal dynamic model from a set of training examples. This approach may be preferred when explicitly modeling all possible nonlinear effects is cumbersome [16].

In previous work [17] we compared an analytical model and two supervised machine learning methods (Least Squares Support Vector Machines and Feedforward Neural Networks) for the estimation of internal forces in the James robotic arm. We performed batch (offline) learning using real data gathered during an exploration phase in which the robot was moving the arm randomly, with different velocities.

In this paper, instead, we perform this estimation online during goal-directed reaching movements. Indeed, retrieving the data while performing meaningful actions (instead of random movements) could be a better strategy in order to limit the exploration to the most useful part of the learning space; this in general can improve learning accuracy and convergence time, as shown for example in [18]. We train online an LWPR neural network [19] during reaching movements directed towards visually identified target objects, manually checking that the robot arm was not subject to any external force; whenever the robot hand was touching the target object, this was detected through the hand tactile sensor, and those data were not used for learning. Data is composed by arm joint positions and velocities ($\mathbf{q}, \dot{\mathbf{q}} \in \mathbb{R}^8$) and measured forces and torques ($\mathbf{x} = [\mathbf{f}^\top, \tau^\top]^\top = \mathbf{x}_I \in \mathbb{R}^6$). We consider only 4 DOFs of the arm (i.e. shoulder and elbow) because the contribution given by the motion of the wrist to the internal dynamics ($\mathbf{x}_I$) is minimal and can be neglected. Moreover, we don't include acceleration measurements ($\ddot{\mathbf{q}}$) as they are too noisy in our setup, and simply worsen the estimation performance; we had evidence of this also in our previous offline learning experiments [17].

The estimation error (NMSE) has been computed on a separated test set of 2000 samples collected during later reaching movements. Results show that the NMSE decreases as more training samples are provided to the learning network: in particular, the NMSE after 1000 samples is 0.18, and after additional movements this error decreases to 0.07 (with 10000 samples).

IV. Experimental Results

A. Force interaction

Given the estimation of the internal forces, the external forces can be obtained as in equation III.3. When reaching for a target object, the information of the FT sensor can now be used to detect the presence of an obstacle that constrains the motion of the robotic arm, and to control an obstacle avoidance motion. The proposed solution uses potential force field [20] for motion generation and Incremental Least Squares Regression [21] to estimate a relation between the measured wrench (due to contact with the obstacle) and the necessary motor command to avoid the obstacle. Such relation, defined here as *Jacobian of the contact* maps the motor velocities to the variation of wrench measured by the FT sensor. The estimation of such relation provides possible directions to avoid the obstacle without the knowledge of the application point of the external wrench along the structure of the robotic arm. In the experiment described in this Section we actuate four DOFs of the arm (i.e. 3 DOFs shoulder and 1 DOF elbow); the arm configuration is defined as $\mathbf{q} = [q1\ q2\ q3\ q4]^T = [\theta_{sp}\ \theta_{sy}\ \theta_{sr}\ \theta_e]^T \in \mathbb{R}^4$.

During a generic unconstrained reaching movement, we define a force field in the robot joint space, where the arm target configuration is an attractive pole. Conversely, any arm configuration which needs to be avoided due to the detection of an obstacle can be modeled as a repulsive pole within the same force field.

Therefore, given a desired target configuration, the attractive pole attracts the arm toward that configuration; a velocity command, proportional to the distance from the target, is given to each joint:

$$\dot{\mathbf{q}}(t) = K_a(\mathbf{q}^a - \mathbf{q}(t)) \tag{IV.1}$$

where $K_a \in \mathbb{R}^{4x4}$ is a constant positive definite gain matrix. While reaching the target configuration, if a contact occurs, the motion of each joint is first blocked and the estimation of the *Jacobian of the contact* is performed by controlling the robot motion by assigning the reference velocities $\dot{\mathbf{q}}$ as:

$$\dot{\mathbf{q}}(t) = -K_c \hat{J}_c(t)^T \mathbf{x}_E(t) \tag{IV.2}$$

where $K_c \in \mathbb{R}^{4x4}$ is a constant positive definite gain matrix. The estimation of the *Jacobian of the Contact* $\hat{J}_c$ is performed as follows:

$$\hat{J}_c(t) = \hat{J}_c(t - \Delta t) + \Delta \hat{J}_c(t) \tag{IV.3}$$

The update of the estimation, $\Delta \hat{J}_c$ is computed as follows:

$$\Delta \hat{J}_c(t) = \frac{\left\{ (\Delta \mathbf{x}_E(t) - \hat{J}_c(t - \Delta t) \Delta \mathbf{q}(t) \right\} \Delta \mathbf{q}(t)^T W(t)}{\varrho + \Delta \mathbf{q}(t)^T W(t) \Delta \mathbf{q}(t)} \tag{IV.4}$$

where $\Delta \mathbf{x}_E(t) \in \mathbb{R}^6$ is the vector of the external forces/torques variations at time t, and $\Delta \mathbf{q}(t) \in \mathbb{R}^4$ is the

vector of arm joints positions variations at time t, W is a weighting matrix and ϱ is a forgetting factor. The arm joint positions, $\mathbf{q}$, and external force/torque measurements, $\mathbf{x}_E$, are used to estimate online the Jacobian of the contact, $\hat{J}_c(t) \in \mathbb{R}^{6x4}$. The controller in Equation IV.2 drives the robot to a safe position (i.e. a position in which both the external forces and torques are equal to zero).

After the external wrench is controlled to be zero, the potential force field is updated adding a repulsive pole at the configuration $\mathbf{q}^r$ in which the contact happened. The presence of a repulsive pole generates a velocity $\dot{\mathbf{q}}$, as in equation IV.5, which is added to the velocity generated by the attractive pole (see Equation IV.1).

$$\dot{\mathbf{q}}(t) = K_r(\mathbf{q}^r - \mathbf{q}(t)) \tag{IV.5}$$

where $K_a \in \mathbb{R}^{4x4}$ is a constant positive definite gain matrix. Now the arm motion is driven by the attractive action of a pole located in the arm target configuration (Eq. IV.1) and by the repulsive action of the new pole (Eq. IV.5). In this way the robot is able to find a safe path to reach for the target without hitting the obstacle.

In Figure 2 a joint-space trajectory followed by the arm during an obstacle avoidance movement is depicted (red solid line). The trajectory is compared to the situation in which the obstacle is not present (blue dashed line). The sensory stimuli that elicited the motor action are shown in Figure 3. Since the evaluation of the external forces and torques is noisy, due to intrinsic sensor noise and internal forces and torques estimation errors, we put arbitrary upper and lower thresholds to determine the presence or not of a contact ($\pm 5N$ for forces and $\pm 1Nm$ for torques). If at least one component of x_E exceeds the threshold, the obstacle avoidance action starts.

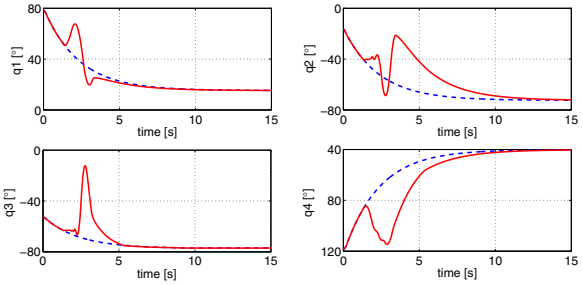

Fig. 2. Arm joints trajectories during an obstacle avoidance movement. The red solid line is the trajectory followed when there is contact with the object. The blue dashed line shows the same movement performed without any contact.

B. Tactile interaction

The tactile information is integrated with vision and external force/torque sensing, triggering different actions depending on those sensory information.

Three sets of graphs describe three different situations that could occur during a ballistic reaching action:

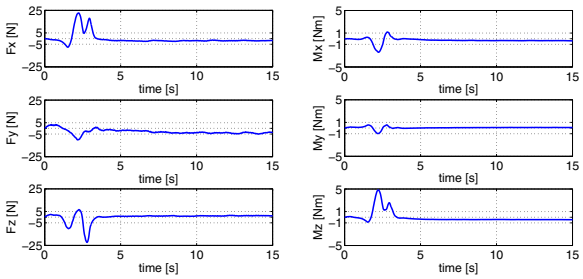

Fig. 3. Estimation of the external forces and torques during the movement. When at least one of the components exceeds the upper or lower threshold the obstacle avoidance motion starts, driven by this information.

. ballistic reaching without any contact between the hand and the external environment. The arm simply moves to the target joints configuration;

. ballistic reaching with contact between the hand and the external environment while the hand is inside the visual field. The touched object is assumed to be the target one; the reaching action is considered to be accomplished successfully and the arm motion stops;

. ballistic reaching with contact between the hand and the external environment while the hand is outside the visual field. The touched object is assumed not to be the target one, and therefore is treated like an obstacle that needs to be avoided; the robot moves the wrist in order to avoid the object (i.e. the obstacle).

Differently from previous section, here we consider an additional DOF of the arm, namely the wrist pitch θ_{wp}. Therefore, the arm configuration is here defined as $\mathbf{q} = [q1\ q2\ q3\ q4\ q5]^T = [\theta_{sp}\ \theta_{sy}\ \theta_{sr}\ \theta_e\ \theta_{wp}]^T \in \mathbb{R}^5$. Anyway, this additional DOF is actually moved only in the third situation, while in the first two cases its position is controlled to zero.

The first set of graphs describes a ballistic reaching action without any hand contact. Figure 4 reports arm joints positions and velocities. The arm is controlled to reach the target joints configuration, which is an attractive pole in the potential field, as described in Section IV-A.

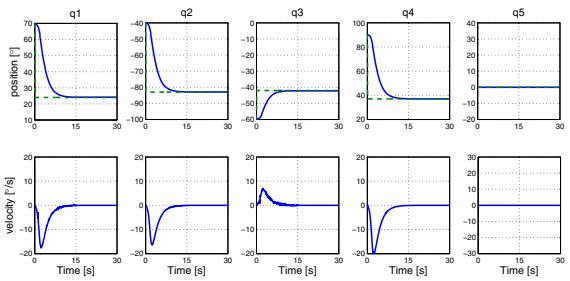

Fig. 4. Arm joints positions and velocities during a ballistic reaching movement. No hand contact occurs.

The second set of graphs describes the situation in which a contact is sensed during the ballistic motion, while the hand is visually detected inside the visual field. This concurrence

of visual and tactile stimulation causes the ballistic motion to suddenly stop, as the target object is considered to be reached.

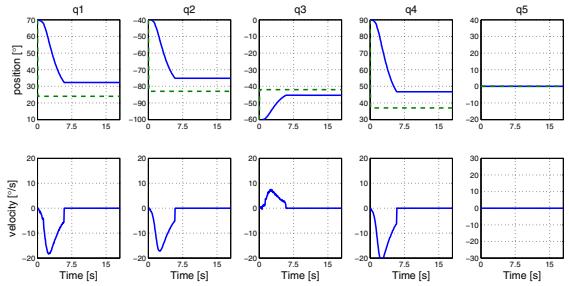

Fig. 5. Arm joints positions and velocities during a ballistic reaching movement. Hand contact occurs while the hand is inside the visual field: the target is considered to be reached and the arm motion suddenly stops.

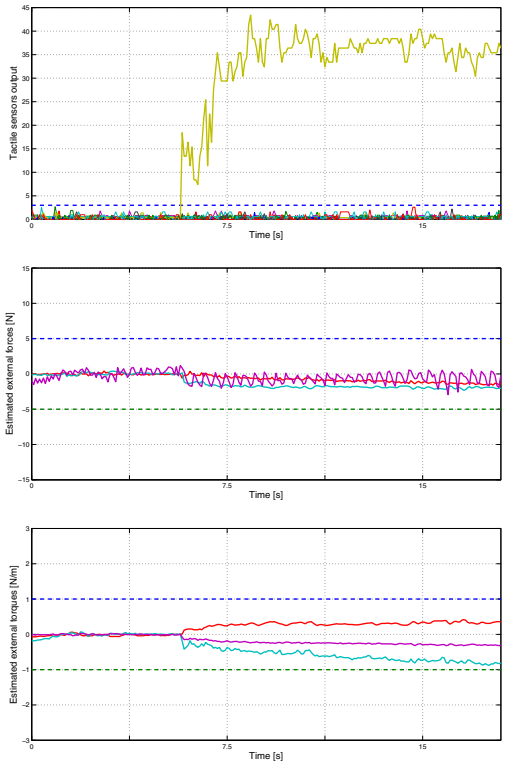

Fig. 6. Ballistic reaching movement in which hand contact occurs while the hand is inside the visual field: the target is considered to be reached and the arm motion suddenly stops. Top: hand tactile sensors measurements. Middle: estimation of external forces. Bottom: estimation of external torques.

It is clear from Figure 5 how the joints positions do not reach the desired value; on the contrary, they all rest at a different position, and all velocities instantaneously go to zero, as soon as one of the tactile sensors outputs exceeds a predifined threshold (see top image in Figure 6); any output under an arbitrary defined threshold (the dashed line in the graph) is ignored, as it is generally due to sensor noise (note that even applying this threshold the sensors are able to detect very slight contacts, in the order of $10^{-1}N$, normal component of the applied force).

The contact of the hand with the object is also reflected in the external forces and torques estimation (middle and bottom images in Figure 6). However, the contact is slight and the estimated forces and torques do not exceed their thresholds (the dashed lines, same as in the previous experiment; see section IV-A and Figure 3). Indeed, the two sensory systems (i.e. FT sensing and tactile sensing) work at different scales. Consequently, no obstacle avoidance motion of the arm is generated. Furthermore, the integration of tactile and visual sensations enriches the perception of external forces/torques: the robot is aware that the contact is happening on the hand (which is also inside the visual field, and probably touching the target object) and can plan its actions on the basis of this more complete information. In this case, no obstacle avoidance motion is needed, since the hand has reached for the target object and the arm motion has been stopped.

Finally, the last set of graphs describes a different situation, in which the contact happens when the hand lies outside the visual field. In this case, the hand is probably not touching the target object, but something else (i.e. an unexpected obstacle). Therefore, the robot should avoid this obstacle while continuing the motion toward the target arm configuration. To achieve this, it can move the wrist trying to cancel the tactile stimulation (i.e. to eliminate the contact). Figure 7 depicts this action. It can be noticed that the motion of the first 4 DOF of the arm is the same as in Figure 4, where no contact was present; conversely, the wrist is moved back to avoid the obstacle (see Figure 7, joint $q5$). Wrist motion is elicited by the tactile sensors stimulation shown in the top image of Figure 8. Remarkably, this time more than one sensor output has exceeded the threshold. In particular, four tactile elements are stimulated in sequence: the first is the *phalangeal-sensor* of the index finger, the second and third are the *phalangeal-sensors* of the middle finger and the last one is the *fingertip-sensor* of the middle finger. This indicates that the hand slithered on the object during the motion. During the interaction the wrist is controlled with a velocity proportional to the intensity of the (overall) tactile stimulation. When there is no contact, wrist position is restored to zero with a proportional controller.

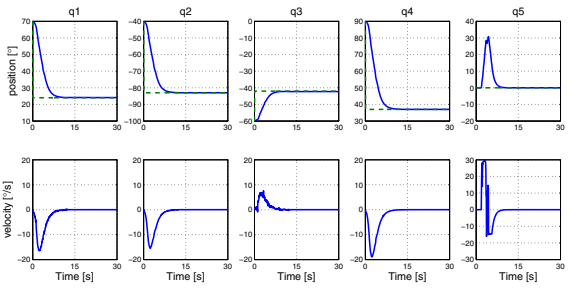

Fig. 7. Arm joints positions and velocities during a ballistic reaching movement. Hand contact occurs while the hand is outside the visual field: an obstacle avoidance movement of the wrist is performed.

Middle and bottom images in Figure 8 plot the estimated external forces and torques. Even in this case, the magnitude

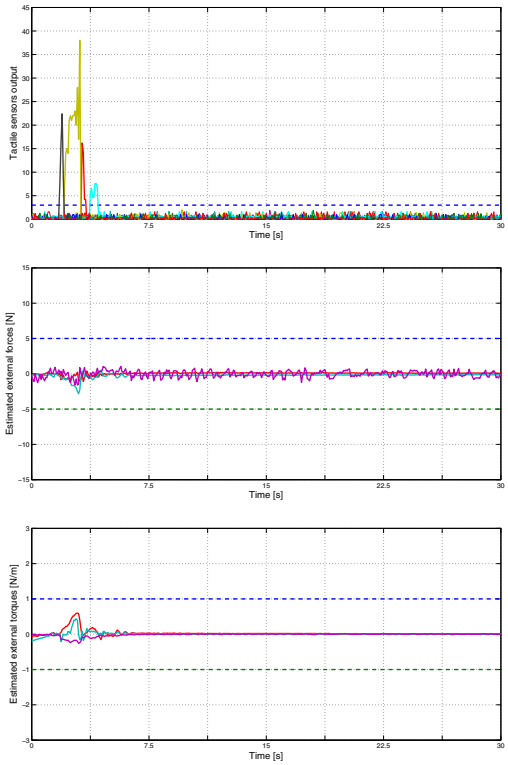

Fig. 8. Ballistic reaching movement in which hand contact occurs while the hand is outside the visual field: an obstacle avoidance movement of the wrist is performed. Top: hand tactile sensors measurements. Middle: estimation of external forces. Bottom: estimation of external torques.

of the estimated external forces/torques during contact is not enough to generate an arm obstacle avoidance action. Since in this case the hand is outside the visual field, and therefore we assume that the hand is in contact with an obstacle (and not with the target object), if the external forces/torques were larger (i.e. exceeding the thresholds) it could have meant that wrist motion was not enough to avoid the touched obstacle, and therefore an obstacle avoidance motion of the arm would have been executed to complete the ballistic reaching successfully and safely (as described in Section IV-A). This strategy exploits the fact that the two sensory sytems (FT and tactile) can detect contacts at different scales.

V. Conclusions

We presented a novel integrated approach to control the interaction of a robotic arm with the external environment through force and tactile sensing; in particular, we described how this integration is realized during visually guided goal-directed reaching. We showed through experimental results obtained with a humanoid robotic platform that the combined use of distributed sensors with different sensitivity allows to deal with different types of contact situations; different control strategies are executed depending on the location and the intensity of the contact, without relying on any a-priori information or modeling of the environment, and they permit to execute visually guided reaching movements successfully and safely, avoiding harmful collisions with unexpected obstacles.

References

[1] A. Albu-Schffer and al., "Anthropomorphic soft robotics - from torque control to variable intrinsic compliance," in *Robotics Research*. Springer Berlin Heidelberg, 2011, pp. 158–207.

[2] B. Vanderborght and al., "Variable impedance actuators: A review," *Robotics and Autonomous Systems*, vol. 61, no. 12, pp. 1601–1614, 2013.

[3] M. Shinya and K. Kazuhiro, "Collision detection system for manipulator based on adaptive impedance control law," in *International Conference on Robotics and Automation (ICRA)*. IEEE, 2003, pp. 1080–1085.

[4] S. Lu, J. H. Chung, and S. A. Velinsky, "Human-robot collision detection and identification based on wrist and base force/torque sensors," in *IEEE International Conference on Robotics and Automation (ICRA)*, April 2005, pp. 3796–3801.

[5] G. Liu, K.Iagnemma, S. Dubowsky, and G. Morel, "A base force/torque sensor approach to robot manipulator inertial parameter estimation," in *IEEE International Conference on Robotics and Automation (ICRA)*, 1998.

[6] M. Fumagalli, M. Randazzo, F. Nori, L. Natale, G. Metta, and G. Sandini, "Exploiting proximal f/t measurements for the icub active compliance," in *Intelligent Robots and Systems (IROS), 2010 IEEE/RSJ International Conference on*. IEEE, 2010, pp. 1870–1876.

[7] M. Fumagalli, "Increasing perceptual skills of robots through proximal force/torque sensors: A study for the implementation of active compliance on the icub humanoid robot," 2013, phD Thesis.

[8] M. Fumagalli, S. Ivaldi, M. Randazzo, L. Natale, G. Metta, G. Sandini, and F. Nori, "Force feedback exploiting tactile and proximal force/torque sensing," *Autonomous Robots*, vol. 33, no. 4, pp. 381–398, 2012.

[9] L. Jamone, F. Nori, G. Metta, and G. Sandini, "James: A humanoid robot acting over an unstructured world," in *International Conference on Humanoid Robots*, Genova, Italy, 2006.

[10] "F/T Sensor Mini45 - ATI Industrial Automation," https://www.ati-ia.com/products/ft/ft_models.aspx?id=Mini45.

[11] L. Jamone, L. Natale, G. Metta, F. Nori, and G. Sandini, "Autonomous online learning of reaching behavior in a humanoid robot," *International Journal of Humanoid Robotics*, vol. 9, no. 3, 2012.

[12] L. Jamone, L. Natale, M. Fumagalli, F. Nori, G. Metta, and G. Sandini, "Machine-learning based control of a human-like tendon driven neck," in *International Conference on Robotics and Automation*. Anchorage, Alaska, USA: IEEE-RAS, 2010.

[13] M. Fumagalli, L. Jamone, G. Metta, L. Natale, F. Nori, A. Parmiggiani, M. Randazzo, and G. Sandini, "A force sensor for the control of a human-like tendon driven neck," in *International Conference on Humanoid Robots*. Paris, France: IEEE-RAS, 2009.

[14] L. Sciavicco and B. Siciliano, *Modeling and control of robot manipulators*. MacGraw-Hill, 1996.

[15] J. Swevers, C. Ganseman, D. B. Tukel, J. D. Schutter, and H. V. Brussel, "Optimal robot excitation and identification," *IEEE Trans. on Robotics and Automation*, vol. 3, no. 5, pp. 730–740, 1997.

[16] J. Ting, M. Mistry, J. Peters, S. Schaal, and J. Nakanishi, "A bayesian approach to nonlinear parameter identification for rigid body dynamics," *Robotics: Science and Systems (RSS)*, 2006.

[17] M. Fumagalli, A. Gijsberts, S. Ivaldi, L. Jamone, G. Metta, L. Natale, F. Nori, and G. Sandini, "Learning how to exploit proximal force sensing: a comparison approach," in *From motor to interaction learning in robots*. Springer-Verlag, 2010.

[18] L. Jamone, L. Natale, K. Hashimoto, G. Sandini, and A. Takanishi, "Learning task space control through goal directed exploration," in *International Conference on Robotics and Biomimetics*. Phuket, Thailand: IEEE-RAS, 2011.

[19] S. Vijayakumar and S. Schaal, "Locally weighted projection regression: An o(n) algorithm for incremental real time learning in high dimensional space," in *International Conference on Machine Learning (ICML)*, 2000, pp. 1079–1086.

[20] O. Khatib, "Real-time obstacle avoidance for manipulators and mobile robots," *The International Journal of Robotics Research*, vol. 5, pp. 90–98, 1986.

[21] K. Hosoda and M. Asada, "Versatile visual servoing without knowledge of true jacobian," in *International Conference on Intelligent Robots and Systems (IROS)*. IEEE, 1994.